IEEE Access
Multidisciplinary | Rapid Review | Open Access Journal

Received November 11, 2018, accepted November 29, 2018, date of publication December 12, 2018,
date of current version February 4, 2019.

Digital Object Identifier 10.1109/ACCESS.2018.2886202

Automatic Leader-Follower Persistent Formation Control for Autonomous Surface Vehicles

C. L. PHILIP CHEN[1,2,3], (Fellow, IEEE), DENGXIU YU[1,4], AND LU LIU[2], (Student Member, IEEE)

[1]Faculty of Science and Technology, University of Macau, Macau 999078, China
[2]College of Navigation, Dalian Maritime University, Dalian 116026, China
[3]State Key Laboratory of Management and Control for Complex Systems, College of Navigation, Institute of Automation, Chinese Academy of Sciences, Beijing 100080, China
[4]Unmanned System Research Institute, Northwestern Polytechnical University, Xi'an 710072, China

Corresponding author: Dengxiu Yu (yudengxiu@126.com)

This work was supported in part by the National Natural Science Foundation of China under Grant 61751202, Grant 61751205, and Grant 61572540, in part by the Key Program for International S and T Cooperation Projects of China under Grant 2016YFE0121200, in part by the Macau Science and Technology Development Fund under Grant 079/2017/A2, Grant 024/2015/AMJ, and Grant 019/2015/A, and in part by the Multiyear Research Grants of the University of Macau.

ABSTRACT This paper presents a novel leader–follower formation control for autonomous surface vehicles (ASVs). The dynamic model of ASV and the traditional methods of trajectory tracking are analyzed. Previous research about ASVs' formation focuses on the way of realizing trajectory tracking under conditions, such as time-delays, finite-time, and non-holonomic system. However, principles of constructing a suitable ASVs formation are often neglected. We present a novel leader–follower relation-invariable persistent formation (RIPF) control for ASVs, from which a persistent formation can be generated in any position. Obtained by using RIPF control potential function, the outputs of RIPF control are data points, which should be smoothened using broad learning system (BLS). The global leader navigates the mission trajectory, and each follower follows the RIPF trajectory to satisfy the RIPF potential function. The neural network-based adaptive dynamic surface control is introduced to solve the mission trajectory tracking problems. Environmental disturbances exist in ASV model, and BLS also can be used to approximate the disturbances. The simulation results show that the proposed generative method and control law are effective to realize the desired formation.

INDEX TERMS Leader-follower, autonomous surface vehicles, trajectory tracking, relation-invariable persistent formation, broad learning system, dynamic surface control.

I. INTRODUCTION

Formation control technology for ASVs plays an increasingly significant role in commerce, science, and especially in marine [1]. Facilitated by new sensor, communication and computer technology, more sophisticated concepts will emerge. The dirty, dull and dangerous environment poses a higher demand of autonomous formation, which consists of autonomous marine craft. The vessels can function as nodes in communication and sensor networks. Ultimately, ASVs can complete possible tasks which cannot be completed by single vehicle caused by the increasing operational robustness.

There are two systems for ASVs formation structure. One is the homogeneous system in which each ASV has the same function and structure. This system is made up of thousands of ASVs with limited ability. Large number of these simple ASVs gather together to generate global dynamical behavior through local interaction. Parallel network structure is suitable for this system. The other is heterogeneous system in which the function and structure of ASVs are not the same. This system includes a limited number of powerful ASVs and some limited ASVs. This system can perform complex tasks which could not be completed by single ASV. Leader-follower network structure is suitable for this system. There are many approaches to formation control [2]. The behavioral virtual structure and leader-follower are the most famous. As for behavioral approach, control action for each vehicle is derived by weighted average of desired behaviors, such as formation keeping, goal seeking and obstacle avoiding. This approach is widely used in decentralized control and the

control strategies can be deduced when robots have multiple objects to complete [3]. As for leader-follower approach [1], [4]–[8], the leader tracks a predefined path and the follower maintains a desired geometric configuration with the leader. The follower can be designated as a leader for another vehicle if necessary. The advantage of this approach is that a single vehicle can direct the group, which is particularly appreciated for its simplicity and scalability. The internal formation stability can be induced by control laws of individual vehicles as the reference trajectory is clearly defined.

During the past few years, the researchers have paid attention to formation control concept and strategy, such as in [9]–[24]. Most of them focus on the control of predefined formation topology but not interpret how to construct the formation topology. As a result, the previous ASVs formation control has the following disadvantages: (a) the predefined formation topology is not suitable for all system and different systems may need different predefined formation topologies; (b) the predefined formation cannot be optimized and its topology is not guaranteed to be the optimum; (c) the predefined formation topology cannot ensure the formation structure valid when some vehicles fail.

RIPF can present a novel formation generation strategy, which provides a suitable formation topology to realize desired behavior and leader-follower. By using potential function, RIPF control drives vehicles arrive its desired formation topology. The reference trajectory in NDSC method must be a smooth function but the output of RIPF control are discrete points, so these discrete points should be fitted to a smooth function. BLS is a novel network architecture, proposed in [25], and it provides an effective and efficient learning framework for modeling nonlinear functions because of its high abilities in function approximation [26], [27]. The drawback of radial basis function NN is that it takes too much time to train abundant parameters in the filters and layers. All the parameters in BLS, by contrast, could be determined by a random projection method. The leader-follower control for ASVs is proposed in [4], [10], and [11], in which the leader would navigate its mission trajectory and each follower would maintain relative position in formation by using the position of the global-leader via an exogenous system. The backstepping technique is introduced to solve a geometric task and a dynamic task of the formation of marine craft. Dynamic surface control is imported into first-order filter to reduce the computational complexity of controller, which is easy for microprocessor system implementation. Each ASV has a relative position to reach, named desired position. Two tasks of ASV control are as follows: to realize the desired formation topology and to navigate the mission trajectory.

Main contributions of this paper can be summarized as follows:

1) RIPF, a new formation generation method for ASVs formation, is presented. It can generate a distance-based formation from any position.
2) A new potential function is designed for RIPF, through which we can get the output of RIPF control that then can be fitted by BLS to a smooth trajectory.
3) We analyze the BLS stability, RIPF control stability, and global stability.

The rest of the paper is as follows. Section II introduces basic information. In Section III, the control module design is analyzed. We analyze the BLS stability, RIPF control stability, and global stability in Section IV. In Section V, we make simulating experiments to test the proposed generation and control of RIPF for ASVs. Based on simulating experiments, conclusions are made in section VI.

II. PRELIMINARIES AND PROBLEM STATEMENT

In the section, we will introduce RIPF, BLS, and problem statement.

A. RIPF [28]

Given a directed graph $G = (V, E)$, $(i, j) \in E$ represents the information transfer from j to i. In other words, i is the follower of j or j is the leader of i. $V = \{1, 2, \ldots, N\}$ is a non-empty vertex set and $E = \{(i, j), i, j \in V, i \neq j\}$ is a directed edge set.

Definition 1: Given an undirected graph $G = (V, E)$ in a plane, G is a relation-invariable minimal rigid graph (RIMRG) if and only if there is a topology that satisfies

$$\begin{cases} \|p_i - p_j\| = c, & \forall (i, j) \in E, \\ p_i \neq p_j, & \forall i,\ j \in V, \\ |E| = 2|V| - 3, \end{cases}$$

where $i \neq j$, p_i is the position vector of the ith vertex, c is a constant, and $|\bullet|$ is the number of elements in set $\bullet$.

P^* denotes the position of vertices satisfying the desired distance set Ψ and T^* is the formation congruent to P^*.

Definition 2: Let $G = (V, E)$ be a RIMRG. By attaching direction to RIMRG, we get a directed graph G_d. The formation T is a RIPF if and only if T can congruent to P^* when the vertices move along the desired direction in G_d, which can be described as

$$T^* \triangleq \{(i, j) \in E : \|p_i^* - p_j^*\| = \varphi_{ij}\}. \tag{1}$$

Fig.1 is an example to illustrate RIPF. In Fig.1, the 5th node is the global-leader and 2nd node is the co-leader. By constructing the rigid matrix M_c, we can judge whether the graph is rigid or not [29]. In Fig.1(a), the rank of rigid matrix $rank(M_c) < 2|V| - 3$, then the graph is flexible and it is not a RIPF. Connecting the edge $(1, 3)$ with the communication direction, a minimal rigid persistent formation is obtained. However, the 1st node has only one leader and the 3rd node has three leaders, which would cause disorder of the communication. Attaching correct direction to RIMRG, we can get a RIPF in Fig.1(c). Adjusting the distance equally, we can obtain the desired equilateral-triangle formation in Fig.1(d).

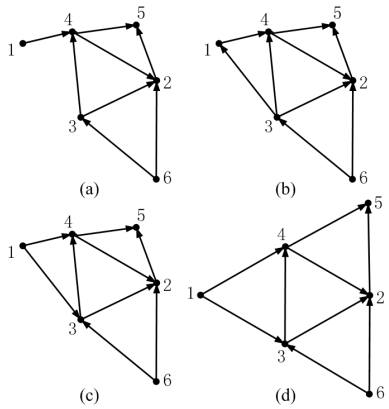

FIGURE 1. Non-RIPF and RIPF.

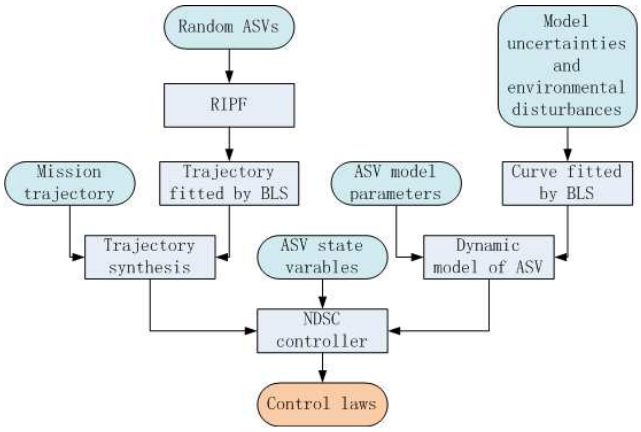

FIGURE 2. The control flow of ASVs formation.

B. BLS

In general neural control system with unknown nonlinearities, the input vector of the approximator is denoted as $X = (x_1, x_2, \cdots, x_M)$ and the desired output is denoted as Y.

We denote the output of the kth feature node in the ith mapping group as [25]

$$F_k^i = \sum_{l=1}^{M}(w_l^k x_l + b_l^k), \tag{2}$$

where w_l^k and b_l^k are the weight and bias term connecting the lth input x_l to the kth feature node respectively. Then the BLS output can be denoted as

$$\hat{y} = \sum_{i=1}^{n} w_i F_i + \sum_{j=1}^{m} w_j \xi_j (\sum_{i=1}^{n} w_j^i F_i + b_j), \tag{3}$$

where w_i is the weight connecting the ith feature node to the output, w_j is the weight connecting the jth enhancement node to the output, ξ_j is the activation function, w_j^i is the weight connecting the ith feature node to the jth enhancement node, and b_j is the bias term related to the jth enhancement node.

The weight matrix, which connects feature nodes and enhancement nodes to the output, is

$$W = ((w_i)_{1\times n}, (w_j)_{1\times m}). \tag{4}$$

We denote $\beta_e = (b_j)_{1\times m}$. We only update W and β_e by gradient descent to retain the random features produced by the feature mapping from inputs. The error function between the actual output y and the model output $\hat{y}$ is defined as follows:

$$E = \frac{1}{2}(y - \hat{y})^2. \tag{5}$$

C. PROBLEM STATEMENT

During the past years, researchers have paid attention to formation control concept and strategy, but the construction of formation topology is mostly ignored. RIPF control for ASVs can present a novel formation strategy, which provides a suitable formation topology to realize desired behavior and leader-follower. The output of RIPF control is non-smooth and then BLS algorithm fits the curve. The global-leader would navigate its mission trajectory and each follower would maintain relative position in formation. The backstepping technique is introduced to solve the geometric task and the dynamic task. The dynamic surface control is introduced to the first-order filter to reduce the computational complexity of controller. The BLS can also be used to approximate model uncertainties and environmental disturbances. Control flow of tasks can be described in Fig.2.

The tracking error of the ith ASV is denoted as ε and the optimal formation control problem can be stated as follows:

$$min \sum_{i=1}^{N}(\varepsilon^T \varepsilon + \sum_{(i,j)\in E}(\|p_i - p_j\| - d_{ij}^{ref})^2), \tag{6}$$

where N is the number of ASVs and d_{ij}^{ref} is the desired distance between i-ASV and j-ASV.

III. CONTROL MODULE DESIGN

In this section, we would analyze the dynamic model of ASV, design of RIPF, and the RIPF control for ASVs formation.

A. DYNAMIC MODEL OF ASV

To describe the kinematic and dynamic model of the ASVs, we define a body-fixed frame $\{X_B, Y_B\}$ and a global coordinate frame $\{X, Y\}$, as shown in Fig.3, and the notations inside are shown in Table 1. In leader-follower RIPF, the global-leader ASV does not follow any other ASVs and the co-leader ASV follows the global-leader ASV only. As shown in Fig.3, each follower follows two leaders and the q_d is the desired position that can satisfy the desired distances φ_1 and φ_2.

Kinematics of a ASV with three degree-of-freedom can be denoted as

$$\begin{cases} \dot{\mathbf{x}} = ucos\psi - vsin\psi, \\ \dot{\mathbf{y}} = usin\psi + vcos\psi, \\ \dot{\psi} = r. \end{cases} \tag{7}$$

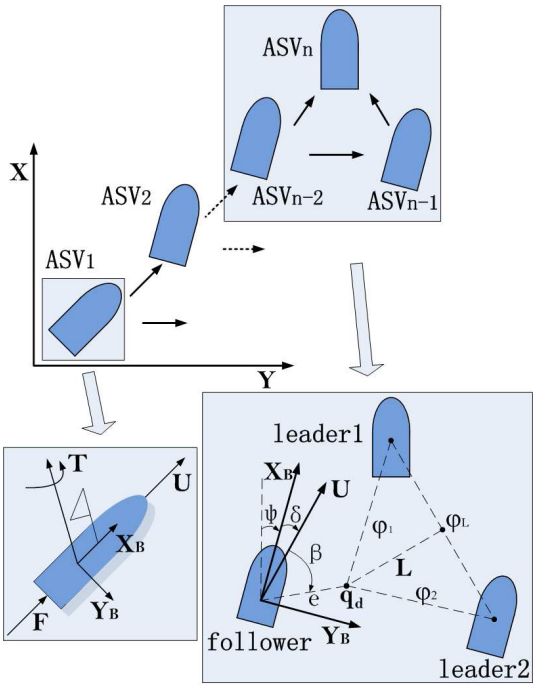

FIGURE 3. The formation of ASVs and ASV model.

TABLE 1. Notations used in this paper.

Symbol	Definition	Symbol	Definition
$\mathbf{x}$	Position in surge	$\mathbf{y}$	Position in sway
ψ	Yaw	u	Linear velocity in surge
v	Linear velocity in sway	r	Yaw velocity
m	Weight of ASV	L	Desired distance
$X_{\dot{u}}$	Added mass in surge	$Y_{\dot{v}}$	Added mass in sway
$N_{\dot{r}}$	Added mass in yaw	d_u	Disturbance in surge
d_v	Disturbance in sway	d_r	Disturbance in yaw
F	Force in surge	T	Moments in yaw
δ	Sideslip angle	e	Tracking error
β	Angle tracking error	φ_i	Distance between ASVs
Symbol	Definition		
X_u	Linear damping coefficients in surge		
Y_v	Linear damping coefficients in sway		
N_r	Linear damping coefficients in yaw		
I_z	Moments of inertia in yaw		

And its dynamics can be denoted as

$$\begin{cases} \dot{u} = \dfrac{m_{22}}{m_{11}}vr - \dfrac{d_{11}}{m_{11}}u + \dfrac{F+d_u}{m_{11}}, \\ \dot{v} = -\dfrac{m_{11}}{m_{22}}ur - \dfrac{d_{22}}{m_{22}}v + \dfrac{d_v}{m_{22}}, \\ \dot{r} = \dfrac{m_{11}-m_{22}}{m_{33}}uv - \dfrac{d_{33}}{m_{33}}r + \dfrac{T+d_r}{m_{33}}, \end{cases} \tag{8}$$

where $m_{11} = m - X_{\dot{u}}$, $m_{22} = m - Y_{\dot{v}}$, $m_{33} = I_z - N_{\dot{r}}$, $d_{11} = -X_u$, $d_{22} = -Y_v$, and $d_{33} = -N_r$.

Let t represent the time variable. Consequently, the inertial position and velocity vectors of the ideal particle are denoted as $q(t) = [\mathbf{x}(t), \mathbf{y}(t)]^T \in R^2$ and $\dot{q}(t) = [\dot{\mathbf{x}}(t), \dot{\mathbf{y}}(t)]^T \in R^2$, respectively. We simplify $q(t), \mathbf{x}(t), \mathbf{y}(t)$ as $q, \mathbf{x}, \mathbf{y}$. The velocity vector is characterized by size and orientation [30]. The size is denoted by $U = (\dot{q}^T\dot{q})^{\frac{1}{2}}$, which represents the speed. The orientation, which is also called azimuth angle, can be represented by the angular variable:

$$\chi = arctan(\frac{\dot{\mathbf{y}}}{\dot{\mathbf{x}}}). \tag{9}$$

Then the geometric path can continuously be parameterized by the time variable t, and the position of its predefined trajectory is denoted as $q_d(t)$. The predefined trajectory of ASV combines the fitting curve obtained by BLS algorithm in RIPF control and the predefined trajectory of global-leader. The formation task is achieved when the followers track their desired position.

The distance between leader vehicle position and desired position is

$$q_d \triangleq q_L + \begin{bmatrix} cos\chi & -sin\chi \\ sin\chi & cos\chi \end{bmatrix} L, \tag{10}$$

where χ is the yaw of follower with respect to the earth-fixed inertial frame and L is the desired distance between the center of two leaders and the desired position of follower with respect to the body-fixed inertial frame q_L.

Tracking error is

$$e \triangleq \sqrt{(\mathbf{x}_d - \mathbf{x})^2 + (\mathbf{y}_d - \mathbf{y})^2}. \tag{11}$$

Angle tracking error is

$$\beta \triangleq tan^{-1}(\frac{\mathbf{y}_d - \mathbf{y}}{\mathbf{x}_d - \mathbf{x}}) - \psi - \delta. \tag{12}$$

As a result, the motion dynamic error can be easily deduced as

$$\begin{cases} \dot{e} = \dot{\mathbf{x}}_d cos\psi_d + \dot{\mathbf{y}}_d sin\psi_d - vsin\beta + 2usin^2(\dfrac{\beta}{2}) - u, \\ \dot{\beta} = -\dfrac{sin\psi_d}{e}\dot{\mathbf{x}}_d + \dfrac{cos\psi_d}{e}\dot{\mathbf{y}}_d + \dfrac{cos\beta}{e}v - \dfrac{sin\beta}{e}u - r - \dot{\delta}, \end{cases} \tag{13}$$

where $\psi_d = tan^{-1}(\frac{\mathbf{y}_d - \mathbf{y}}{\mathbf{x}_d - \mathbf{x}})$. In order to stabilize the dynamic error, we present the virtual control laws as follows:

$$\begin{cases} \alpha_u = k_1\bar{e} + \dot{\mathbf{x}}_d cos\psi_d + \dot{\mathbf{y}}_d sin\psi_d - vsin\beta + 2usin^2(\dfrac{\beta}{2}), \\ \alpha_r = k_2\beta - \dfrac{sin\psi_d}{e}\dot{\mathbf{x}}_d + \dfrac{cos\psi_d}{e}\dot{\mathbf{y}}_d + \dfrac{cos\beta}{e}v - \dfrac{sin\beta}{e}u - \dot{\delta}, \end{cases} \tag{14}$$

where $k_1 > 0$, $k_2 > 0$ and $\bar{e} = e - \epsilon$ (ϵ can avoid the singularity of α_r). In this virtual control laws, the sideslip angle is compensated and the influence upon the cross velocity swerving is avoided. Using the first-order-filter and dynamic surface control to filter α_u and α_r, we can get two new variances z_u and z_r:

$$\begin{cases} \gamma_1\dot{z}_u + z_u = \alpha_u, \quad z_u(0) = \alpha_u(0), \\ \gamma_2\dot{z}_r + z_r = \alpha_r, \quad z_r(0) = \alpha_r(0), \end{cases} \tag{15}$$

where γ_1 and γ_2 are the filter time constants.

The linear velocities in surge error and yaw velocity error are

$$\begin{cases} e_u \triangleq z_u - u, \\ e_r \triangleq z_r - r. \end{cases} \tag{16}$$

Differentiating (16) yields the following error dynamic:

$$\begin{cases} m_{11}\dot{e}_u = m_{11}\dot{z}_u + f_1 - F, \\ m_{33}\dot{e}_r = m_{33}\dot{z}_r + f_2 - T, \end{cases} \tag{17}$$

where

$$\begin{cases} f_1 = -m_{22}vr + d_{11}u - d_u, \\ f_2 = -(m_{11} - m_{22})uv + d_{33}r - d_r. \end{cases} \tag{18}$$

We can see that environment disturbance exists in f_1 and f_2, and it can be approximated by BLS as follows:

$$\begin{cases} f_1 = \sum_{i=1}^{n} w_i^1 F_i^1 + \sum_{j=1}^{m} w_j^1 \xi_j^1 (\sum_{i=1}^{n} w_j^{i,1} F_i^1 + b_j^1), \\ f_2 = \sum_{i=1}^{n} w_i^2 F_i^2 + \sum_{j=1}^{m} w_j^2 \xi_j^2 (\sum_{i=1}^{n} w_j^{i,2} F_i^2 + b_j^2). \end{cases} \tag{19}$$

Consequently, the dynamic control laws are

$$\begin{cases} F = -m_{11}\dot{e}_u + m_{11}\dot{z}_u + f_1, \\ T = -m_{33}\dot{e}_r + m_{33}\dot{z}_r + f_2. \end{cases} \tag{20}$$

B. DESIGN OF RIPF

To generate RIPF, we design the generative method of RIPF, which is described in Algorithm 1.

Algorithm 1 The Generative Method of RIPF

Require: ASVs in random position
Ensure: ASVs RIPF
1: Generate the Delaunay Triangulation from random position;
2: Delete boundary edges under the condition that residue graph is rigid;
3: Change special edges under the condition that residue graph is rigid;
4: Attach direction to edges.

The ASVs would be driven to arrive their desired positions when the RIPF is generated. The desired RIPF can be found by solving the problem of distance-based formation, which can be figured out by the gradient control law. One contribution of this paper is to derive a new potential function for ASVs formation. We model the motion of the vehicles as first-order integrators,

$$\dot{p}_i = -\nabla_{p_i} G_i, \tag{21}$$

where p_i and G_i represent the position and potential function of the ith vehicle respectively.

$(i, j) \in E$ denotes that (i, j) is an edge of edge set E and φ_{ij} represents the desired distance of edge (i, j). We denote $\Psi = \{\varphi_{ij}^2\} \in \mathbb{R}^{N\times N}$ as the distance constraint matrix and $\varphi_{ij} = 0$ when $(i, j) \notin E$.

We denote relative position vector as $\phi_{ij} = p_i - p_j$ when $(i, j) \in E$. The edge matrix is denoted as $\Phi = \{\phi_{ij}\} \in \mathbb{R}^{N\times N}$ and $\phi_{ij} = 0$ when $(i, j) \notin E$.

We denote the desired RIPF as $T^* = (G^*, P^*)$, where $G^* = (V^*, E^*)$. The desired formation in (21) is defined as the set of realizations which are congruent to P^*

$$E_p^* := \{p \in R^{2N} : \|p_i - p_j\| = \|p_i^* - p_j^*\|, (i, j) \in E\}, \tag{22}$$

where $\|p_i^* - p_j^*\| = \varphi_{ij}$.

We set S_q as the neighbors of the qth ASV. The procedure of finding out the coincidence avoidance vertex set E_{sv} is shown in Algorithm 2.

Algorithm 2 Find Out Coincidence Avoidance Vertex Set

Require: The RIPF $G = (V, E)$
Ensure: A coincidence avoidance vertex set
1: Construct an empty set E_{sv};
2: **for** i=1:$|E|$ **do**
3: $p = E(i, 1)$ and $q = E(i, 2)$;
4: **if** $S_p \cap S_q = \{p, q\}$ *or* $S_p \cap S_q = \{q, p\}$ **then**
5: Construct an edge $S_V = (S_p \cap S_q)$;
6: Add S_V to E_{sv};
7: **end if**
8: **end for**

For $\forall(i, j) \in E$, we can get the measured distance $|p_i - p_j|$. Leaders of the ith vehicle is denoted as L^i and its number is denoted as $|L^i|$. Similarly, L_{sv}^i can be obtained through E_{sv}.

There are two parts for the distance error potential function of ith vehicle. Part one is G_i^d and it is the difference between the desired distance φ and the measured distance value ϕ. The other part is G_i^p and it is the penalty function to avoid any vehicle colliding and coinciding with the other vehicles.

$$\begin{cases} G_i = k_a G_i^d + k_b G_i^p, \\ G_i^d = \sum_{j=1}^{|L^i|} ||\phi_{ij} - \varphi_{ij}||, \quad j \in L^i, \\ G_i^p = \sum_{j=1}^{|L_{sv}^i|} ||(p_i - p_j) - (p_i^* - p_j^*)||, \quad j \in L_{sv}^i, \end{cases} \tag{23}$$

where $k_a > 0$ and $k_b > 0$ are variances that should be designed.

RIPF control realizes the desired formation topology by using the potential function. However, the reference trajectory in NDSC method should be a smooth function and the output of RIPF control are data points, which should be smoothed by using BLS. The trajectory of rth ASV can be denoted as

$$q_r(t) = \sum_{i=1}^{n} w_i^r F_i^r + \sum_{j=1}^{m} w_j^r \xi_j^r (\sum_{i=1}^{n} w_j^{i,r} F_i^r + b_j^r). \tag{24}$$

C. RIPF CONTROL FOR ASVS FORMATION

Based on RIPF, the ASVs formation is composed of the track of the planned trajectory and that of the RIPF trajectory. The global-leader of the formation is the only one to track the predefined trajectory and the others track the target trajectory. Position of the planned trajectory is denoted as $q_p(t) \in R^2$. RIPF trajectory of the rth ASV is denoted as $q_r(t) \in R^2$. Consequently, target trajectory of the rth ASV can be denoted as

$$q_r^{ref}(t) = q_p(t) + q_r(t). \tag{25}$$

IV. STABILITY ANALYSIS

A. BLS STABILITY

We set the activation function as follows:

$$\xi_j = \frac{e^x - e^{-x}}{e^x + e^{-x}}. \tag{26}$$

Derivative of activation function can be obtained:

$$\dot{\xi}_j = 1 - \xi_j^2. \tag{27}$$

From (5), we can deduce the following derivatives:

$$\begin{cases} \dfrac{\partial E}{\partial w_i} = \dfrac{\partial E}{\partial \hat{y}} \cdot \dfrac{\hat{y}}{\partial w_i} = (\hat{y} - y)F_i, \\ \dfrac{\partial E}{\partial w_j} = \dfrac{\partial E}{\partial \hat{y}} \cdot \dfrac{\hat{y}}{\partial w_j} = (\hat{y} - y)\xi_j(\sum\limits_{i=1}^{n} w_j^i F_i + b_j), \\ \dfrac{\partial E}{\partial w_j^i} = \dfrac{\partial E}{\partial \hat{y}} \cdot \dfrac{\hat{y}}{\partial \xi_j} \cdot \dfrac{\partial \xi_j}{\partial w_j^i} \\ \qquad = (\hat{y} - y)w_j F_i(1 - \xi_j^2(\sum\limits_{i=1}^{n} w_j^i F_i + b_j))), \\ \dfrac{\partial E}{\partial b_j} = \dfrac{\partial E}{\partial \hat{y}} \cdot \dfrac{\hat{y}}{\partial \xi_j} \cdot \dfrac{\partial \xi_j}{\partial b_j} \\ \qquad = (\hat{y} - y)w_j(1 - \xi_j^2(\sum\limits_{i=1}^{n} w_j^i F_i + b_j))). \end{cases}$$

The iterative update laws for weight w_i, w_j, w_j^i and bias b_j can be expressed as:

$$\begin{cases} w_i(t+1) = w_i(t) - \eta_1 \dfrac{\partial E}{\partial w_i}, \\ w_j(t+1) = w_j(t) - \eta_1 \dfrac{\partial E}{\partial w_j}, \\ w_j^i(t+1) = w_j^i(t) - \eta_1 \dfrac{\partial E}{\partial w_j^i}, \\ b_j(t+1) = b_j(t) - \eta_1 \dfrac{\partial E}{\partial b_j}, \end{cases} \tag{28}$$

where η_1 is the learning rate of BLS.

We set

$$x \triangleq \|y - \hat{y}\|.$$

Then the potential function, $f(x)$, of BLS becomes

$$f(x) = x. \tag{29}$$

Based on the approximation formula of total differential, we have

$$\nabla f(x_t) \approx \nabla P[\frac{\partial x_t}{\partial P}]^T,$$

where $P \triangleq [w_i, w_j, w_j^i, b_j]$.

To realize the asymptotic stability, we have that:

$$\begin{aligned} \|x_{t+1}\|^2 &= \|x_t - \eta_1 \nabla f(x_t)\|^2 \\ &= \|x_t\|^2 - 2\eta_1 \nabla f(x_t)^T x_t + \eta_1^2 \|\nabla f(x_t)\|^2, \end{aligned} \tag{30}$$

where η_1 is the learning rate of BLS gradient descent control.

Based on Lipschitz conditions, we can deduce that:

$$f(x_t) - f(0) \leq \nabla f(x_t)^T (x_t - 0) + \frac{1}{2\beta_1} \|\nabla f(x_t) - \nabla f(0)\|^2, \tag{31}$$

where β_1 is a real constant that satisfies $\beta_1 \geq 0$.

Suppose 0 is the optimal solution, we obtain $\nabla f(0) = 0$ and $f(x_t) \geq f(0)$. Then we have that:

$$-\nabla f(x_t)^T x_t \leq \frac{1}{2\beta_1} \|\nabla f(x_t)\|^2. \tag{32}$$

Then, (30) becomes

$$\begin{aligned} \|x_{t+1}\|^2 &\leq \|x_t\|^2 - \frac{\eta_1}{\beta_1} \|\nabla f(x_t)\|^2 + \eta_1^2 \|\nabla f(x_t)\|^2 \\ &= \|x_t\|^2 - \eta_1 (\frac{1}{\beta_1} - \eta_1) \|\nabla f(x_t)\|^2. \end{aligned} \tag{33}$$

Obviously, we can deduce that $\|x_{t+1}\|^2 < \|x_t\|^2$ under the condition that $\eta_1 < \frac{1}{\beta_1}$ and x_t will converge to 0. Thus the BLS is an effective method to fit the trajectory by using the output in RIPF control.

B. RIPF STABILITY

Ref to Definition 1, there is a desired distance set X^* for any RIPF to realize. We set

$$\begin{cases} n = |E|, \\ x_{ij} \triangleq (\|p_i - p_j\| - d_{ij}^{ref})^2, \end{cases}$$

where (i, j) is an edge in E. Then the potential function, $f(x_{ij})$, of RIPF becomes

$$f(x_{ij}) = \sum_{(i,j) \in E} x_{ij}. \tag{34}$$

x_{ij} is a time-varying variable and can be denoted as x_t. To realize the asymptotic stability, we have

$$\begin{aligned} \|x_{t+1}\|^2 &= \|x_t - \eta_2 \nabla f(x_t)\|^2 \\ &= \|x_t\|^2 - 2\eta_2 \nabla f(x_t)^T x_t + \eta_2^2 \|\nabla f(x_t)\|^2, \end{aligned} \tag{35}$$

where η_2 is the learning rate of RIPF gradient descent control.

Based on Lipschitz conditions, we can deduce that:

$$f(x_t) - f(0) \leq \nabla f(x_t)^T (x_t - 0) + \frac{1}{2\beta_2} \|\nabla f(x_t) - \nabla f(0)\|^2, \tag{36}$$

where β_2 is a real constant that satisfies $\beta_2 \geq 0$. Suppose 0 is the optimal solution, we have $\nabla f(0) = 0$ and $f(x_t) \geq f(0)$. Then we have that:

$$-\nabla f(x_t)^T x_t \leq \frac{1}{2\beta_2}\|\nabla f(x_t)\|^2. \tag{37}$$

Then, (35) becomes

$$\begin{aligned}\|x_{t+1}\|^2 &\leq \|x_t\|^2 - \frac{\eta_2}{\beta_2}\|\nabla f(x_t)\|^2 + \eta_2^2\|\nabla f(x_t)\|^2 \\ &= \|x_t\|^2 - \eta_2(\frac{1}{\beta_2} - \eta_2)\|\nabla f(x_t)\|^2. \end{aligned}\tag{38}$$

Obviously, we can deduce that $\|x_{t+1}\|^2 < \|x_t\|^2$ under the condition that $\eta_2 < \frac{1}{\beta_2}$ and x_t will converge to 0.

C. ASYMPTOTIC STABILITY FOR ASVS FORMATION

From (6), we can see that $\hat{y}_j$ would be adjusted to realize

$$min \sum_{(i,j)\in E} (\|p_i - p_j\| - d_{ij}^{ref})^2,$$

which does not affect the stability of $\varepsilon^T\varepsilon$. The stability of RIPF control is proved above and the stability of control law which is to realize $min\ \varepsilon^T\varepsilon$ is proved as follows.

Variables of dynamic model can be transformed as follows:

$$\begin{cases} x_1 = [\mathbf{x}, \mathbf{y}, \psi, u, v, r]^T, \\ f_0(x_1) = \begin{bmatrix} ucos\psi - vsin\psi \\ usin\psi + vcos\psi \\ r \\ \frac{m_{22}}{m_{11}}vr - \frac{d_{11}}{m_{11}}u \\ -\frac{m_{11}}{n_{22}}ur - \frac{d_{22}}{m_{22}}v \\ \frac{m_{11}-m_{22}}{m_{33}}uv - \frac{d_{33}}{m_{33}}r \end{bmatrix}, \\ f_1(x_1) = [0, 0, 0, \frac{d_u}{m_{11}}, \frac{d_v}{m_{22}}, \frac{d_r}{m_{33}}]^T, \\ U = [0, 0, 0, \frac{F}{m_{11}}, 0, \frac{T}{m_{33}}]^T. \end{cases}$$

Then the dynamic model of ASV can be rewritten as

$$\dot{x}_1 = f_0(x_1) + f_1(x_1) + U. \tag{39}$$

Define the variances in BLS as:

$$\begin{cases} \Xi(t) \triangleq \xi_j(\sum_{i=1}^{n} w_j^i(t)F_i + b_j(t)), \\ \zeta(x_1) = \begin{bmatrix} F_i \\ \Xi(t) \\ w_j(t)F_i(1 - \Xi^2(t)) \\ w_j(t)(1 - \Xi^2(t)) \\ (w_j^i w_j(t)F_i + b_j w_j(t))(1 - \Xi^2(t)) \end{bmatrix}, \\ \hat{\theta} \triangleq [w_i, w_j, w_j^i, b_j, -1]. \end{cases} \tag{40}$$

Let the error surface be

$$S_1 = x_1 - y_r, \tag{41}$$

where y_r is the desired trajectory.

Based on (39) and (41), we get

$$\dot{S}_1 = U + f_0 + f_1 - \dot{y}_r. \tag{42}$$

Based on NDSC technique, we have

$$\dot{S}_1 = -k_1 S_1 - \tilde{\theta}^T\zeta(x_1) + \delta_1^*. \tag{43}$$

Define the estimation error as

$$\tilde{\theta} = \hat{\theta} - \theta^*, \tag{44}$$

where θ^* is the vector that contains ideal weight and bias. The update law for BLS is

$$\dot{\hat{\theta}} = -\eta S_1\zeta(x_1), \tag{45}$$

where $\eta = [\eta_1, \eta_1, \eta_1, \eta_1, 0]$ is the learning rate.

Given a compact set $\Omega_{x_1} \in R^1$ and a coefficient vector $\tilde{\alpha}_j$, let $\theta^* = [\tilde{w}_i, \tilde{w}_j, \tilde{w}_j^i, \alpha_j\tilde{b}_j]$ be the ideal constant weights and the ideal constant bias. Then we have

$$f_1(x_1) = \theta^*\zeta(x_1) + \delta_1^*, \tag{46}$$

where $|\delta_1^*| < \delta_m$, $x_1 \in \Omega_{x_1}$, $\tilde{w}_j^i F_i = -\tilde{\alpha}_j\tilde{b}_j$.

Firstly, we define the positive definite and radially unbounded control Lyapunov Function:

$$V = \frac{1}{2}(S_1^2 + \tilde{\theta}^T\tilde{\theta}). \tag{47}$$

The derivative of the Lyapunov function is:

$$\begin{aligned}\dot{V} &= vS_1\dot{S}_1 + \tilde{\theta}^T\dot{\hat{\theta}} \\ &\leq S_1\delta_1^* - k_1S_1^2 - \tilde{\theta}^TS_1\zeta(x_1) + \tilde{\theta}^T\dot{\hat{\theta}} \\ &= S_1\delta_1^* - k_1S_1^2 - \tilde{\theta}^T(S_1\zeta(x_1) - \dot{\hat{\theta}}). \end{aligned}\tag{48}$$

Substituting the update law (45) into (48) yields

$$\begin{aligned}\dot{V} &\leq S_1\delta_1^* - k_1S_1^2 - \tilde{\theta}^T(S_1\zeta(x_1) + \eta S_1\zeta(x_1)) \\ &= S_1\delta_1^* - k_1S_1^2 - (1+\eta)\tilde{\theta}^TS_1\zeta(x_1). \end{aligned}\tag{49}$$

Choose $k_1 = 1+\alpha_0$ and set $\Lambda = S_1\zeta(x_1)$. Then (49) becomes

$$\begin{aligned}\dot{V} &\leq S_1\delta_1^* - S_1^2 - \alpha_0S_1^2 - (1+\eta)\tilde{\theta}^T\Lambda \\ &\leq \frac{1}{4}\delta_1^{*2} - \alpha_0S_1^2 - (1+\eta)\tilde{\theta}^2 - \frac{1+\eta}{4}\Lambda^2 \\ &\leq \frac{1}{4}\delta_1^{*2} - \alpha_0S_1^TS_1 - \frac{1+\eta}{\beta}\tilde{\theta}^T\tilde{\theta}, \end{aligned}\tag{50}$$

where β is a real constant that satisfies $\beta \geq \nabla f_1(x_1)$.

There is $\{\alpha_0 \leq \frac{1+\eta}{\beta}, \alpha_0 \in (0, 1)\}$ if $1 + \eta < \beta$.

Noting that $|\delta_1^*| < \delta_m$, we can deduce

$$\begin{aligned}\dot{V} &< -\alpha_0(S_1^TS_1 + \tilde{\theta}^T\tilde{\theta}) + \frac{1}{4}\delta_m^2 \\ &= -2\alpha_0V + \frac{1}{4}\delta_m^2. \end{aligned}\tag{51}$$

Function $V(t)$ is a continuous function, and $V(t) \geq 0$ with $t > 0$. If

$$\dot{V}(t) \leq -k_1V(t) + k_2 \tag{52}$$

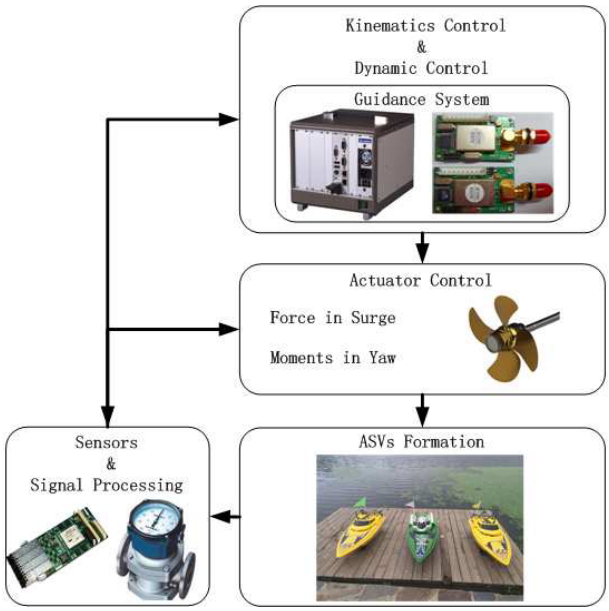

FIGURE 4. The motion control hierarchy of ASVs formation.

where k_1 and k_2 are positive constants, then

$$V(t) \leq V(0)e^{-k_1 t} + \frac{k_2}{k_1}(1 - e^{-k_1 t}) \tag{53}$$

Asymptotic stability for ASVs formation is proved [31].

V. SIMULATION

The motion control hierarchical structure of ASVs formation is shown in Fig.4. ASVs motion control system is composed of sensor and signal processing, kinematics control, dynamic control, actuator control, and execution of ASVs formation. Autonomy-enabling technology is represented by all the involved building blocks and fully autonomous operation poses a higher demand of additional control levels. The role of so-called kinematic control level is to prescribe ASV velocity commands which is needed to achieve motion control objectives. Kinematics control takes only the geometrical aspects of motion into consideration but it does not refers to forces and moments. Next, dynamic controllers determine the vehicle motion generative method by forces and moments. Designed by NDSC, these controllers can be operated in conditions of parametric uncertainties and environmental disturbances. As for ASVs, they must actively change its direction to follow the velocities ordered by guidance module. Distributed by the control alloction, various ASVs can be controlled by their own control instruction. The execution of ASVs formation is composed of the actuator controllers. The execution can ensure that the actuators behave as required and as a result the ASV can move as prescribed by the guidance laws.

In this section, we testify the analysis of RIPF control for ASVs with simulation results. The x-axis and the y-axis in the simulation are the position coordinate. Parameters of the controller are set as follows: $k_1 = 2$, $k_2 = 2$, $\gamma_1 = 0.2$, $\gamma_2 = 0.2$, $k_a = 1$, $k_b = 1$, $m_{11} = 2376kg$, $m_{22} = 3949kg$, $m_{33} = 3584kg$, $d_{11} = (12 + 2.5|u|)kg/s$, $d_{22} = (17 + 4.5|v|)kg/s$, $d_{33} = (0.5 + 0.1|r|)kg/s$.

A. RIPF CONTROL

Firstly, a random position set of 6 ASVs in a plane is generated randomly by using Gaussian distribution and the points in Fig.5(a) denote the ASVs. Then we can get the RIPF through Algorithm 1 with edge set $E = \{(1, 6), (2, 5), (2, 6), (3, 4), (3, 6), (4, 1), (4, 6), (5, 1), (5, 6)\}$. Using the gradient of potential function of RIPF control, we can get the RIPF trajectory. Tracking the RIPF trajectory, we can get the desired formation in Fig.5(b), where the scale is enlarged to fit the RIPF trajectory.

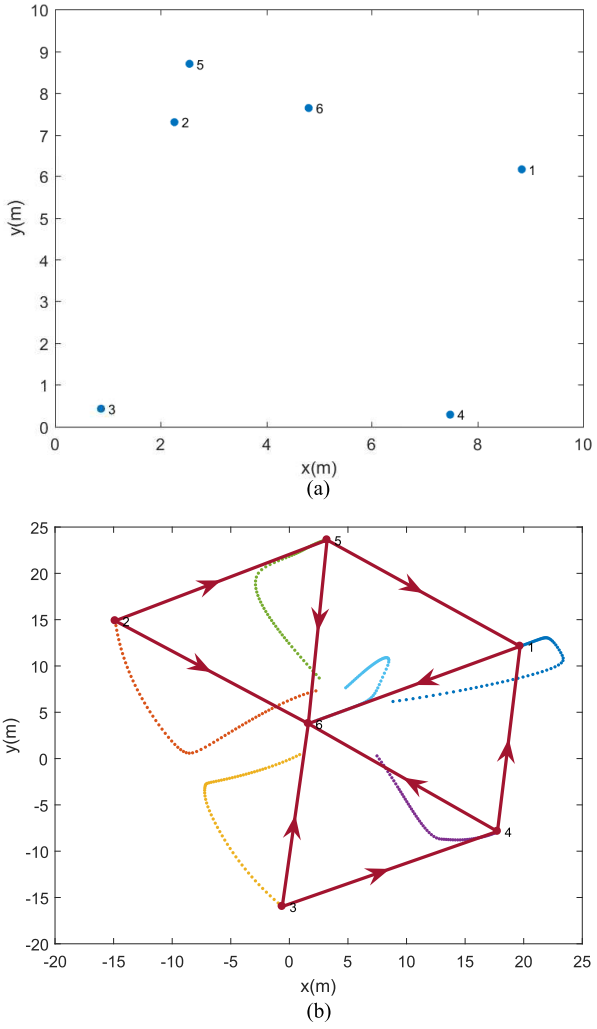

FIGURE 5. Random points and desired formation.

B. THE TRAJECTORY FITTED THROUGH BLS

As presented in previous section, the entire design procedure is followed by particularizing the BLS structure step by step. The BLS with 5 feature nodes and 5 enhancement nodes is used. We set $\eta_1 = 1$.

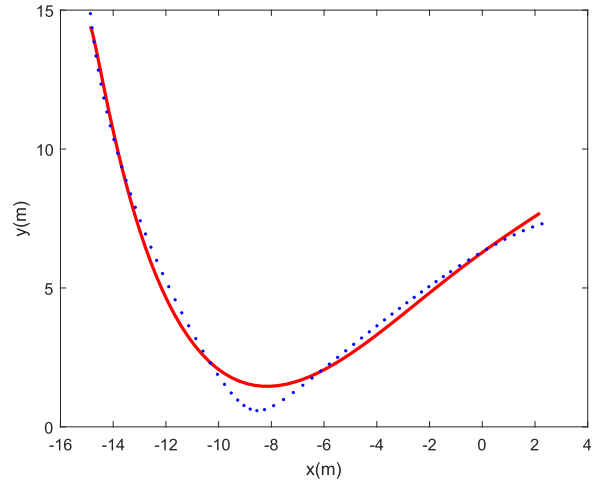

FIGURE 6. The trajectory fitted through BLS.

The input positions of ASVs can be obtained through RIPF control. The input positions are plotted points in Fig.6 and they can be trained so as to get BLS as curve.

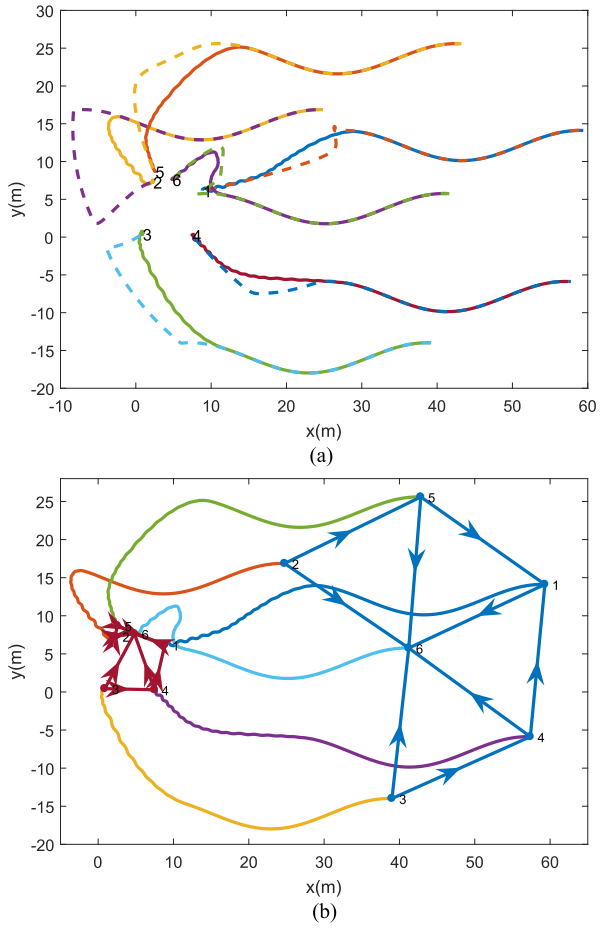

FIGURE 7. Desired target trajectory, actual trajectory and real-time ASVs formation keeping.

C. ASVS FORMATION CONTROL BASED ON RIPF

As shown in Fig.7(a), we can get the desired target trajectory (dotted line) and actual trajectory (solid line). The desired formation can be remained in the process of tracking trajectory in Fig.7(b).

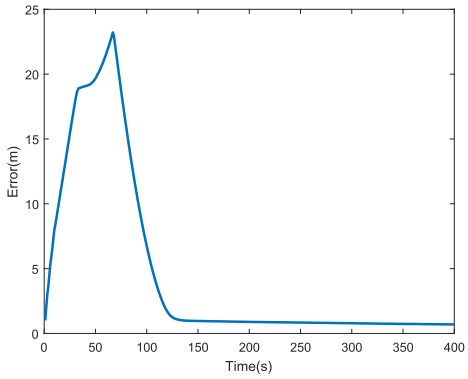

FIGURE 8. The sum of tracking error.

As shown in Fig.8, the sum of tracking error firstly increases and then decreases. Since the angle tracking error is large at the beginning, the tracking error would increase. The sum of tracking error would never be zero because of the tracking time bias.

VI. CONCLUSION

The paper presents a novel leader-follower formation control, called RIPF control for autonomous surface vehicles. RIPF is a novel formation strategy, which can realize its desired formation topology by using the potential function. The output of RIPF is smoothed by BLS algorithm. The global-leader navigates the mission trajectory and each follower maintains its place in formation. The tracking task of trajectory is solved by NDSC. Simulations show that random-position ASVs can successfully generate its RIPF, RIPF can converge to its desired formation and ASVs can also realize real-time formation keeping during the process of moving.

REFERENCES

[1] R. Cui, S. S. Ge, B. V. E. How, and Y. S. Choo, "Leader–follower formation control of underactuated autonomous underwater vehicles," *Ocean Eng.*, vol. 37, nos. 17–18, pp. 1491–1502, Dec. 2010.
[2] M. Breivik, V. E. Hovstein, and T. I. Fossen, "Ship formation control: A guided leader-follower approach," *IFAC Proc. Vol.*, vol. 41, no. 2, pp. 16008–16014, 2008.
[3] S. Monteiro and E. Bicho, "A dynamical systems approach to behavior-based formation control," in *Proc. IEEE Int. Conf. Robot. Autom.*, vol. 3, May 2002, pp. 2606–2611.
[4] C.-E. Ren, L. Chen, and C. L. P. Chen, "Adaptive fuzzy leader-following consensus control for stochastic multiagent systems with heterogeneous nonlinear dynamics," *IEEE Trans. Fuzzy Syst.*, vol. 25, no. 1, pp. 181–190, Feb. 2017.
[5] K.-K. Oh and H.-S. Ahn, "Leader-follower type distance-based formation control of a group of autonomous agents," *Int. J. Control, Autom. Syst.*, vol. 15, no. 4, pp. 1738–1745, Aug. 2017.
[6] W. Ni and D. Cheng, "Leader-following consensus of multi-agent systems under fixed and switching topologies," *Syst. Control Lett.*, vol. 59, nos. 3–4, pp. 209–217, Mar./Apr. 2010.

[7] L. Ding, Q.-L. Han, and G. Guo, "Network-based leader-following consensus for distributed multi-agent systems," *Automatica*, vol. 49, no. 7, pp. 2281–2286, Jul. 2013.
[8] K. Shojaei, "Leader–follower formation control of underactuated autonomous marine surface vehicles with limited torque," *Ocean Eng.*, vol. 105, pp. 196–205, Sep. 2015.
[9] Z. Lin, L. Wang, Z. Han, and M. Fu, "Distributed formation control of multi-agent systems using complex Laplacian," *IEEE Trans. Autom. Control*, vol. 59, no. 7, pp. 1765–1777, Jul. 2014.
[10] Y.-K. Zhu, X.-P. Guan, and X.-Y. Luo, "Finite-time consensus of heterogeneous multi-agent systems with linear and nonlinear dynamics," *Acta Automat. Sinica*, vol. 40, no. 11, pp. 2618–2624, 2014.
[11] X. Dong, J. Xiang, L. Han, Q. Li, and Z. Ren, "Distributed time-varying formation tracking analysis and design for second-order multi-agent systems," *J. Intell. Robotic Syst.*, vol. 86, no. 2, pp. 277–289, May 2017.
[12] T. H. Summers, C. Yu, S. Dasgupta, and B. D. O. Anderson, "Control of minimally persistent leader-remote-follower and coleader formations in the plane," *IEEE Trans. Autom. Control*, vol. 56, no. 12, pp. 2778–2792, Dec. 2011.
[13] W. Ren and Y. Cao, *Distributed Coordination of Multi-Agent Networks: Emergent Problems, Models, and Issues*. London, U.K.: Springer-Verlag, 2011.
[14] S. Sui, C. P. Chen, and S. Tong, "Neural network filtering control design for nontriangular structure switched nonlinear systems in finite time," *IEEE Trans. Neural Netw. Learn. Syst.*, 2018.
[15] X. Luo, X. Li, S. Li, Z. Jiang, and X. Guan, "Flocking for multi-agent systems with optimally rigid topology based on information weighted Kalman consensus filter," *Int. J. Control, Autom. Syst.*, vol. 15, no. 1, pp. 138–148, Feb. 2017.
[16] L. Liu, D. Wang, Z. Peng, and T. Li, "Modular adaptive control for LOS-based cooperative path maneuvering of multiple underactuated autonomous surface vehicles," *IEEE Trans. Syst., Man, Cybern., Syst.*, vol. 47, no. 7, pp. 1613–1624, Jul. 2017.
[17] L. Liu, D. Wang, and Z. Peng, "ESO-based line-of-sight guidance law for path following of underactuated marine surface vehicles with exact sideslip compensation," *IEEE J. Ocean. Eng.*, vol. 42, no. 2, pp. 477–487, Apr. 2017.
[18] Z. Peng, D. Wang, Y. Shi, H. Wang, and W. Wang, "Containment control of networked autonomous underwater vehicles with model uncertainty and ocean disturbances guided by multiple leaders," *Inf. Sci.*, vol. 316, no. 20, pp. 163–179, Sep. 2015.
[19] G. Lai, Z. Liu, Y. Zhang, C. L. P. Chen, S. Xie, and Y. Liu, "Fuzzy adaptive inverse compensation method to tracking control of uncertain nonlinear systems with generalized actuator dead zone," *IEEE Trans. Fuzzy Syst.*, vol. 25, no. 1, pp. 191–204, Feb. 2017.
[20] F. Wang, Z. Liu, Y. Zhang, and C. L. P. Chen, "Adaptive fuzzy control for a class of stochastic pure-feedback nonlinear systems with unknown hysteresis," *IEEE Trans. Fuzzy Syst.*, vol. 24, no. 1, pp. 140–152, Jan. 2016.
[21] G. Wen, C. L. P. Chen, Y.-J. Liu, and Z. Liu, "Neural network-based adaptive leader-following consensus control for a class of nonlinear multiagent state-delay systems," *IEEE Trans. Cybern.*, vol. 47, no. 8, pp. 2151–2160, Aug. 2017.
[22] T. Gao, Y.-J. Liu, L. Liu, and D. Li, "Adaptive neural network-based control for a class of nonlinear pure-feedback systems with time-varying full state constraints," *IEEE/CAA J. Autom. Sinica*, vol. 5, no. 5, pp. 923–933, Sep. 2018.
[23] L. Liu, D. Wang, Z. Peng, and H. H. T. Liu, "Saturated coordinated control of multiple underactuated unmanned surface vehicles over a closed curve," *Sci. China Inf. Sci.*, vol. 60, no. 7, p. 070203, 2017.
[24] H. Xiao, Z. Li, and C. L. P. Chen, "Formation control of leader–follower mobile robots' systems using model predictive control based on neural-dynamic optimization," *IEEE Trans. Ind. Electron.*, vol. 63, no. 9, pp. 5752–5762, Sep. 2016.
[25] C. L. P. Chen and Z. L. Liu, "Broad learning system: An effective and efficient incremental learning system without the need for deep architecture," *IEEE Trans. Neural Netw. Learn. Syst.*, vol. 29, no. 1, pp. 10–24, Jan. 2018.
[26] J. Zhou, C. L. P. Chen, L. Chen, and H. X. Li, "A collaborative fuzzy clustering algorithm in distributed network environments," *IEEE Trans. Fuzzy Syst.*, vol. 22, no. 6, pp. 1443–1456, Dec. 2014.
[27] C. L. P. Chen and Y.-H. Pao, "An integration of neural network and rule-based systems for design and planning of mechanical assemblies," *IEEE Trans. Syst., Man, Cybern.*, vol. 23, no. 5, pp. 1359–1371, Sep. 1993.
[28] D. Yu and C. L. P. Chen, "Automatic leader-follower persistent formation generation with minimum agent-movement in various switching topologies," *IEEE Trans. Cybern.*, to be published.
[29] X.-Y. Luo, S.-B. Li, and X.-P. Guan, "Automatic generation of min-weighted persistent formations," *Chin. Phys. B*, vol. 18, no. 8, p. 3104, 2009.
[30] L. Wang, Z. Han, and Z. Lin, "Realizability of similar formation and local control of directed multi-agent networks in discrete-time," in *Proc. IEEE 52nd Annu. Conf. Decis. Control (CDC)*, Dec. 2013, pp. 6037–6042.
[31] D. Wang and J. Huang, "Neural network-based adaptive dynamic surface control for a class of uncertain nonlinear systems in strict-feedback form," *IEEE Trans. Neural Netw.*, vol. 16, no. 1, pp. 195–202, Jan. 2005.

C. L. PHILIP CHEN (S'88–M'88–SM'94–F'07) graduated from the University of Michigan at Ann Arbor, Ann Arbor, MI, USA. He is currently a Chair Professor with the Department of Computer and Information Science, Faculty of Science and Technology, University of Macau, Macau, China. The University of Macau's Engineering and Computer Science programs receiving the Hong Kong Institute of Engineers' (HKIE) accreditation and Washington/Seoul Accord is his utmost contribution to engineering/computer science education for Macau, as the former Dean of the Faculty.

His current research interests include systems, cybernetics, and computational intelligence. He is a Fellow of AAAS, IAPR, the Chinese Association of Automation (CAA), and HKIE. He was the Chair of the TC 9.1 Economic and Business Systems of International Federation of Automatic Control, from 2015 to 2017, and a Program Evaluator of the Accreditation Board of Engineering and Technology Education of USA for computer engineering, electrical engineering, and software engineering programs. He received the 2016 Outstanding Electrical and Computer Engineers award from his alma mater, Purdue University. He is the Editor-in-Chief of the IEEE TRANSACTIONS ON SYSTEMS, MAN, AND CYBERNETICS: SYSTEMS and an Associate Editor of several IEEE TRANSACTIONS. From 2012 to 2013, he was the IEEE SMC Society President. He is currently the Vice President of CAA.

DENGXIU YU received the bachelor's degree in mechanical design manufacture and automation and the M.S. degree in mechatronic engineering from Northwestern Polytechnical University, Shaanxi, China, in 2013 and 2016, respectively. He is currently pursuing the Ph.D. degree with the University of Macau, Macau, China. His current research interests include formation generation and consensus control of multiagent systems.

LU LIU (S'16) received the B.E. degree in electrical engineering and automation and the Ph.D. degree in marine electrical engineering from Dalian Maritime University, Dalian, China, in 2012 and 2018, respectively.

She is currently a Lecturer with Dalian Maritime University. Her current research interests include guidance and control for marine surface vessels and adaptive control.